PHYSICAL REVIEW A VOLUME 24, NUMBER 3 SEPTEMBER 1981

Equation of state of dense, partially degenerate, reacting plasmas

F. J. Rogers
University of California, Lawrence Livermore National Laboratory, Livermore, California 94550
(Received 20 April 1981)

A method is presented for treating ionization equilibrium in the presence of plasma coupling, which allows for the fact that heavy ions may be strongly coupled (liquidlike) while electrons are only moderately coupled (gaslike). The theory utilizes a many-body perturbation expansion of the grand canonical partition function. Three distinct renormalizations are required to handle the general problem. They account for (1) formation of electron-nucleus composites, (2) coupling of the composite particles to the plasma, and (3) strong coupling of multiply charged heavy ions. Five dimensionless parameters, which are the ratios of two lengths, are required to define the limits of applicability of the theory. Equation-of-state calculations for Ar have been carried out. Corrections to the Saha equation are found to be significantly smaller than predicted by the Debye-Hückel theory. At moderate density this is due to decreased net Coulomb attraction. At high density core repulsion tends to offset (or exceed) the Coulomb attraction term.

I. INTRODUCTION

The equation of state of plasmas has been an active research area for many years. Early research was based on analogy with dissociative equilibrium in molecular gases which have an ideal limit for very low densities. This met with immediate difficulties since ionic and atomic bound-state partition functions are nonconvergent. Various *ad hoc* methods for cutting off the divergence were introduced. The first successful calculation of nonideal effects was made in 1923 by Debye and Hückel,[1] whose interest was in electrolytic solutions. Subsequent workers added the Debye-Hückel, weak coupling, free energy to the ideal plasma model free energy. The ionization state and thermodynamic properties were then obtained by free-energy minimization. A summary and exhaustive list of references of work prior to 1966 is given by Brush.[1] A review and list of references through 1975 is given in the monograph by Ebeling, Kraeft, and Kremp.[2]

Owing to the analytical complexity of a rigorous treatment of nonideal plasmas most of the literature cited in the above review articles is concerned with hydrogen. These results are very important to our fundamental understanding but have limited applications. Besides being restricted to $Z=1$, they are also limited to low density. Several recent attempts to treat slightly nonideal plasmas for arbitrary Z and all stages of ionization have been given.[3,4] These are based on free-energy minimization procedures which require some assertions as to how individual atoms and ions can be uncoupled from the plasma. In the present paper we avoid making these assertions by working in the grand canonical formalism or what Krasnikov[5] calls the "physical model." Furthermore, high-Z plasmas for which the ions are very nonideal, while the electrons are moderately nonideal, will be treated.

The limits of applicability of the quantum statistical theory of reacting plasmas to be presented in this work can be described with five dimensionless parameters, which are the ratios of two lengths:

(1) The plasma parameter

$$\Lambda_{ij}=l_{ij}/\lambda_D, \tag{1}$$

where $l_{ij}=\beta\xi_i\xi_j$ is the Landau length for collisions between ions i and j, ξ_i and ξ_j are the corresponding net charges,

$$\lambda_D=\left(4\pi\beta\sum_i \xi_i^2 z_i\right)^{-1/2} \tag{2}$$

is the plasma screening length in the grand canonical ensemble, z_i is the activity for species i given by

$$z_i=(2s_i+1)\,\lambda_i^{-3}e^{\mu_i/kT} \tag{3}$$

and $\lambda_i=(2\pi\hbar^2/m_i kT)^{1/2}$ is the thermal de Broglie wavelength. At low density where the particle motion is weakly correlated $z_i\to\rho_i$, so that $\lambda_D\to\lambda_d$, the usual weak-coupling Debye screening length.

(2) The diffraction parameter

$$\gamma_{ij}=\chi_{ij}/\lambda_D, \tag{4}$$

where $\chi_{ij}=(\hbar^2/2\mu_{ij}kT)^{1/2}$ is the thermal de Broglie wavelength in relative coordinates.

(3) The screening overlap parameter

$$\tau=\bar{r}/\lambda_D, \tag{5}$$

where $\bar{r}$ is the mean ionic core radius.

(4) The degeneracy parameter

$$\theta_e=(\chi_e/a_e)^3, \tag{6}$$

where $a_e=(3/4\pi\rho_e)^{1/3}$ is the electron sphere radius.

(5) The packing parameter,

$$x=(R/a)^3, \tag{7}$$

where R is the effective temperature-dependent hard-core radius, $a=(3/4\pi\rho_{\text{ions}})^{1/3}$ is the ion sphere radius, and ρ_{ions} is the total ion number density.

Since the heavy-ion interactions are classical it is possible to treat ion-ion terms in all orders of perturbation. However, due to the complications introduced by quantum mechanics it is difficult to treat electron-electron and electron-ion interactions beyond screened two-body collision terms. This introduces the restrictions

$$\Lambda_{ee}\leq 1, \quad \Lambda_{ei}\leq 1.$$

The large distance divergences for the Coulomb virial coefficients are classical. Nevertheless, the many-body diagrammatic resummations that remove these divergences introduce some short distance quantum modifications to the screened potential that vanish as $\gamma_{ij}\to 0$. In the present analysis only the leading corrections in γ_{ij} are included which introduces the restriction $\gamma_{ij}\leq 0.5$. The screened interaction potentials are also modified by the presence of bound electrons when λ_D is the same order of magnitude as the ionic size, which introduces the restriction $\tau<1$. Electron degeneracy also has a direct effect on the screened potentials but this does not cause any particular difficulty. However, other effects of degeneracy and exchange are complicated and as a result it is assumed in the present work that $\theta_e\leq 1$. Another restriction that enters the analysis is that $x\leq 0.15$. This results from the fact that core interaction terms are included only in the second virial coefficient. The temperature-dependent hard-sphere radius of multiply charged ions is small compared to the distance of closest approach, so that the core interaction terms are generally only significant for low degrees of ionization. Screened long-range ion-ion interactions are included (approximately) for all virial coefficients.

II. THEORETICAL METHOD

Part of the theoretical basis for the present work has been reported previously.[6-10] In Secs. II A–II D we give a brief summary of previous work, then describe in Secs. II E and II F some new work on strong ion coupling and electron degeneracy.

A. The density expansion

The neglect of the uncertainty principle causes the electron-ion terms to diverge as $r\to 0$, and it is obvious at the outset that reacting plasmas must be treated quantum mechanically. This type of divergence is most important for few body terms. A more pervasive type of divergence occurs in all virial and cluster coefficients for Coulomb systems in the limit $r\to\infty$. This divergence is essentially classical and can only be removed through many-body summation procedures. Each contribution to the many-body sum has small quantum modifications for $r<\chi_{ij}$. As a result, in order to remove the few-body electron-ion divergencies, it is possible to carry out the many-body analysis classically and then insert Slater sums at the appropriate places in the final result. This procedure is rigorous provided γ_{ij} is small compared to 1. Correction terms in powers of γ_{ij} are added at a later stage of the analysis, but for many applications these terms are small.

To obtain the desired density expansion we follow the work of Abe[11] who showed for the classical one-component plasma model (OCP) that the long-range divergences can be eliminated by appropriate reorganizations in powers of the potential (βu). The leading term in the resultant expression for S is the familiar Debye-Hückel correction. Higher-order terms resemble virial coefficients for the screened Coulomb potential. Since the interest here is in real multicomponent plasmas it was necessary to carry out a multicomponent generalization of Abe's work. After the appropriate introduction of quantum mechanics this yields the equation of state of a nonideal completely ionized Boltzmann gas according to

$$(F-F_0)/VkT=-S, \tag{8}$$

$$\frac{P}{kT}=\sum_\nu \rho_\nu + S - \sum_\nu \rho_\nu \frac{\partial S}{\partial \rho_\nu}, \tag{9}$$

where

$$S=S_R+\sum_{ij} S_{ij}+\sum_{ijk} S_{ijk}+\cdots, \tag{10}$$

$$S_R=1/12\pi\lambda_d^3, \quad \lambda_d=\left(4\pi\beta\sum_i \xi_i^2\rho_i\right)^{-1/2}, \tag{11}$$

$$S_{ij}=-\rho_i\rho_j\left[B_{ij}(T,\lambda_d) + 2\pi\int_0^\infty r^2 dr\left(\beta V_{ij}-\frac{(\beta V_{ij})^2}{2}\right)\right], \tag{12}$$

$$V_{ij}=\xi_i\xi_j e^{-r/\lambda_d}/rkT, \tag{13}$$

ν, i, j, k range over all components, and $B_{ij}(T,\lambda_d)$ is the second virial coefficient for the Debye potential V_{ij}. Owing to their large mass the B_{ij} for heavy ions can be calculated classically. If

one or more of the interacting particles is an electron the B_{ij} must be calculated quantum mechanically. Expressions for the higher S_n, where the bar is used to indicate multicomponent structure, are given in Ref. 8. These expressions are valid both classically and quantum mechanically provided $\gamma_{ij}<1$. In order to use Eqs. (8) and (9) to calculate the equation of state for incomplete ionization it is necessary to make assertions as to how composite particles enter the ideal-gas free energy F_0 and the S function. The resulting expressions can then be used to minimize the free energy with respect to changes in the composition.[4]

B. The activity expansion

Since ionization equilibrium is naturally included in the grand canonical ensemble it is the fundamentally correct way to treat this aspect of the problem. Unfortunately, it is subject to all the divergences present in the canonical ensemble and other more complicated divergences as well. In order to avoid the difficulties associated with summing specific types of diagrams a global approach to the problem is taken. This is to find a method for generating the activity expansion as a function of S, thereby obtaining a divergence free expression for P/kT in the grand canonical ensemble. Leading terms in the two-component activity expansion are given by[6-8]

$$\frac{P}{kT}=z_e+z_\alpha+S+\frac{z_e}{2}\left(\frac{\partial S}{\partial z_e}\right)^2+\frac{z_\alpha}{2}\left(\frac{\partial S}{\partial z_\alpha}\right)^2+\cdots, \tag{14}$$

where the subscript e indicates electrons, the subscript α indicates heavy ions of charge Ze, and $S(\rho_e,\rho_\alpha)$ in Eq. (10) has been replaced by $S(z_e,z_\alpha)$. All the classically irreducible diagrams are included in S while all the reducible diagrams are included in the terms involving S two or more times. At equilibrium Eq. (14) must satisfy the conditions

$$n_e=z_e\frac{\partial(P/kT)}{\partial z_e},\quad n_\alpha=z_\alpha\frac{\partial(P/kT)}{\partial z_\alpha}. \tag{15}$$

C. Generalized cluster coefficients

No hint of composite particles has yet entered the analysis. The S function (in the activity) involves virial coefficients for a potential having the Debye exponential form, i.e., Eq. (13) with λ_d replaced by λ_D. In order to properly treat ionization equilibrium it is necessary to collect all the bound-state terms that contribute to each power of the activity, so that all $\underline{n}$ body terms are properly grouped, and thus obtain the cluster coefficients for the exponentially screened potential, e.g., for an ordinary gas $z^3b_3=z^3(-B_3/2+2B_2^2)$. In the special case of a Coulomb gas it is necessary to introduce generalized cluster coefficients. In this case the two- and three-body cluster coefficients are[8] (for two components)

$$C_{\underline{2}}\equiv S_{\underline{2}}=z_e^2s_{ee}+2z_ez_\alpha s_{e\alpha}+z_\alpha^2s_{\alpha\alpha}, \tag{16}$$

$$C_{\underline{3}}\equiv S_{\underline{3}}+\frac{z_e}{2!}\left(\frac{\partial S_{\underline{2}}}{\partial z_e}\right)^2+\frac{z_\alpha}{2!}\left(\frac{\partial S_{\underline{2}}}{\partial z_\alpha}\right)^2, \tag{17}$$

where

$$S_{\underline{3}}=z_e^3s_{eee}+3z_e^2z_\alpha s_{ee\alpha}+3z_ez_\alpha^2s_{e\alpha\alpha}+z^3s_{\alpha\alpha\alpha}$$

and

$$s_{ijk\cdots}\equiv S_{ijk\cdots}/z_iz_jz_k\cdots.$$

For activity (density)-independent potentials the generalized cluster coefficients have the property

$$C_{\underline{n}}\to z^nb_{\underline{n}}. \tag{18}$$

The reorganized form of Eq. (14), through terms in $\frac{5}{2}$ powers of the activity, is [see Eq. (28) of Ref. 8]

$$\frac{P}{kT}=\sum_i z_i+S_R+\sum_i z_i\left(\frac{\partial S_R}{\partial z_i}\right)^2+\sum_i z_i\frac{\partial}{\partial z_i}z_i\left(\frac{\partial S_R}{\partial z_i}\right)^3+\sum_{i\neq j}z_iz_j\left(\frac{\partial S_R}{\partial z_i}\right)\left(\frac{\partial S_R}{\partial z_j}\right)\left(\frac{\partial^2S_R}{\partial z_iz_j}\right)+C_{\underline{2}}+\sum_i z_i\left(\frac{\partial S_R}{\partial z_i}\right)\left(\frac{\partial C_{\underline{2}}}{\partial z_i}\right), \tag{19}$$

where in the present work $i,j=\{e,\alpha\}$.

D. Renormalized activity expansion

The procedure for incorporating composite particles into the activity expansion rests on the observation that the formation of bound states, when kT is less than the binding energy, lowers the order of the cluster coefficients. For example, due to its exponential temperature dependence the bound-state part of the electron-ion second cluster coefficient $b_{e\alpha}$ enters the cluster expansion like a new ideal particle, while the continuum-state part enters like a real two-body interaction between electrons and ions. Because of this it is necessary to introduce an augmented set of activity variables, such that the leading term in the revised activity series corresponds to a modified Saha ionization equilibrium equation.[8] Scattering states are systematically included in the interaction corrections of the reordered activity series, i.e., proper treatment of bound clusters requires the decomposition of the n-body trace into bound and scattering parts.

It is clear that weakly bound clusters do not act

like particles so that some part of the bound-state partition function properly should be included with the scattering-state contribution. It has been shown that the well-known compensation between bound and scattering states leads naturally to a proper decomposition procedure.[9,10] The resulting effective bound-state sum is convergent and there is no need to invoke any cutoff criteria as was done in early work on this problem. For example, the two-body cluster term is separated as follows:

$$C_{e\alpha} \equiv S_{e\alpha} = S^b_{e\alpha} + S^c_{e\alpha}, \tag{20}$$

where

$$S^b_{e\alpha} = z_e z_\alpha \sqrt{2}\, \lambda^3_{e\alpha} \left(\sum_{nl} (2l+1) e^{-E_{nl}/kT} - \omega_0 + \omega_1 \right), \tag{21}$$

$$S^c_{e\alpha} = z_e z_\alpha \sqrt{2}\, \lambda^3_{e\alpha} \left(\frac{1}{\pi} \int_0^\infty \sum_l (2l+1) dp \frac{\partial \delta_l}{\partial p} e^{-p^2/2\mu_{e\alpha} kT} + \omega_0 - \omega_1 \right) + 2\pi \lambda_D^2 \left(\frac{\xi_e \xi_\alpha}{kT} \right) - \frac{\pi}{2} \lambda_D \left(\frac{\xi_e \xi_\alpha}{kT} \right)^2, \tag{22}$$

$$\omega_0 \equiv \sum_{nl} (2l+1), \quad \omega_1 = \sum_{nl} (2l+1) \frac{E_{nl}}{kT}. \tag{23}$$

The two leading terms in the bound-state high-temperature expansion are included with the scattering-state contribution. This is because these terms almost precisely cancel similar terms in the scattering-state part of the trace.[5,9,10] The resulting convergent quantity in the parentheses of Eq. (21) is commonly referred to as the Planck-Larkin partition function.[2]

At this point it has been shown how to identify composite particle contributions in the activity expansion, but only in the pseudoideal gas limit. To go further it is necessary to reorganize the terms so that those terms that correspond to composite particles enter the interaction correction similar to fundamental particles; e.g., the plasma screening length given by Eq. (2) must be transformed according to

$$\lambda_D (z_e + Z^2 z_\alpha) \to \lambda^*_D (z_e + Z^2 z_\alpha + (Z-1)^2 z_{e\alpha} + \cdots), \tag{24}$$

where $z_{e\alpha}$ is the activity for one-electron composites. The first step in this process is to use Eq. (21) to define an activity for one-electron composites according to

$$S^b_{e\alpha}(\lambda_D) \equiv e^{\Lambda_{e\alpha}} z_{e\alpha}. \tag{25}$$

When $\Lambda_{e\alpha} < 1$, a useful expansion is

$$S^b_{e\alpha}(\lambda_D) = (1 + \Lambda_{e\alpha} + \Lambda^2_{e\alpha}/2 \cdots) z_{e\alpha}. \tag{26}$$

Since $\Lambda_{e\alpha}$ depends on the activity according to $z^{1/2}$, terms in the expansion of $\exp(\Lambda_{e\alpha})$ go together, with similar terms in Λ_{ee} and Λ_{ii} appearing elsewhere in the S expansion, and give rise to the transformation of the screening length indicated above.[8] A result of this is that the energy levels that enter the definition of $z_{e\alpha}$ are the shifted Debye energy levels for the screening length λ_D, i.e.,

$$z_{e\alpha} = 2 z_e z_\alpha \left(2^{1/2} \lambda^3_{e\alpha} \sum_{nl} (2l+1) [e^{-E^s_{nl}/kT} - (\omega_0 - \omega_1) e^{-\Lambda_{e\alpha}}] \right), \tag{27}$$

where

$$E^s_{nl}(\lambda^*_D) = E_{nl}(\lambda^*_D) - Ze^2/\lambda^*_D. \tag{28}$$

The renormalized cluster expansion that is obtained is formally similar to Eq. (19) except, due to the fact that the bound states are screened, some additional terms appear. The lowest-order term in this new expansion is equivalent to a Saha equation with a screened Planck-Larkin bound-state partition function.[3] Due to the expansion in terms of Λ_{ij} the resulting equations, as a practical matter, are only applicable when $\Lambda_{ij} < 1$. When $Z \gg 1$, it is generally also true that $\Lambda_{\alpha\alpha} = Z^2 e^2/kT\lambda^*_D \gg 1$, so that the perturbation expansion procedure being discussed here will be inadequate for highly ionized plasmas. A procedure for including strong ion coupling is now presented.

E. Strong heavy-ion coupling

1. The canonical partition function

The interest in this section is to treat strong heavy-ion coupling and ionization equilibrium simultaneously. These two effects, as already described, are most naturally handled by the grand canonical partition function. However, before studying the activity expansion for strongly coupled systems it is instructive to consider the canonical partition function subject to the conditions

$$\lambda_{e\alpha}/\lambda_d < 1, \quad kT \geq Z^2 \text{ Ry}, \quad Z > 1 \tag{29}$$

where Z is the atomic number of an α-type ion. The first condition ensures that the many-body part of the problem is nearly classical, the second condition ensures that there are few bound clusters, and the third condition ensures that the heavy ions are more strongly coupled than the electrons. Moderate electron-ion coupling re-

quires the further condition that the density be low enough that

$$\Lambda_{\rho,ee} < \Lambda_{\rho,e\alpha} < 1 , \tag{30}$$

where $\Lambda_{\rho,ij} = l_{ij}/\lambda_d$ is the plasma parameter in the canonical ensemble which is a function of density rather than activity.

Explicitly writing out the components of Eq. (8) for two- and three-body particle terms gives

$$\begin{aligned}(F - F_0)/VkT = -[&S_R + (\rho_e^2 s_{ee} + 2\rho_e\rho_\alpha s_{e\alpha} + \rho_\alpha^2 s_{\alpha\alpha}) \\ &+ (\rho_e^3 s_{eee} + 3\rho_e^2\rho_\alpha s_{ee\alpha} + 3\rho_e\rho_\alpha^2 s_{e\alpha\alpha} \\ &+ \rho_\alpha^3 s_{\alpha\alpha\alpha}) + \cdots] ,\end{aligned} \tag{31}$$

where $s_{ijk\cdots} \equiv S_{ijk\cdots}/(\rho_i\rho_j\rho_k\cdots)$. It is easy to verify that for each set of n particle terms that the term involving only heavy ions is larger than any of the other terms in the set, e.g., S_{ee} and $S_{e\alpha}$ are given approximately by the three-rung-ladder term[10,12]

$$S_{ij} = \rho_i\rho_j \frac{(\beta\xi_i\xi_j)^3}{12}\left(\ln\frac{\chi_{e\alpha}}{\lambda_d} + 0.887\right) , \tag{32}$$

while $S_{\alpha\alpha}$ is given by the high-density classical limit[13]

$$S_{\alpha\alpha} = \rho_\alpha^2 \pi\lambda_d^3\Lambda_{\rho,\alpha\alpha}^2/2 = \frac{\rho_\alpha}{8}\left(\frac{Z^2\rho_\alpha}{\rho_e + Z^2\rho_\alpha}\right)\Lambda_{\rho,\alpha\alpha} . \tag{33}$$

Since $\beta < Z^2$ Ry it is clear that $S_{\alpha\alpha} > S_{e\alpha} > S_{ee}$ when $Z > 1$. A systematic expansion is therefore obtained by first summing all the terms involving only heavy ions, then all those terms involving one electron and $n-1$ heavy ions, etc.

Adding together all heavy-ion terms gives

$$S_{LT} = \rho_\alpha\Lambda_{\rho,\alpha\alpha}/3 + \rho_\alpha^2 s_{\alpha\alpha} + \rho_\alpha^3 s_{\alpha\alpha\alpha} + \cdots , \tag{34}$$

where S_{LT} is the leading term in the new expansion. Equation (34) $\to S_{OCP}$, the one-component-plasma result, as $Z \to \infty$, since $\lambda_d \to (4\pi\beta e^2 Z^2\rho_\alpha)^{-1/2}$. The first term on the right in Eq. (34) is the direct heavy-ion part of S_R, i.e., $S_R(\rho_e, \rho_\alpha) = (\rho_e\Lambda_{\rho,ee} + \rho_\alpha\Lambda_{\rho,\alpha\alpha})/6$. When the conditions (22) prevail the total free energy is given approximately by

$$(F - F_0)/VkT = -(S_{LT} + \rho_e\Lambda_{\rho,ee}/3 + S_{ee} + 2S_{e\alpha}) . \tag{35}$$

For small and intermediate values of the charge S_{LT} differs appreciably from S_{OCP}, but the Abe method[11] can be applied. This is numerically complicated and consequently simple, accurate, fitting functions have been developed. By studying numerical results[6,13] for $S_{\alpha\alpha}$ and $S_{\alpha\alpha\alpha}$ it was found that

$$\begin{aligned}S_{\alpha\alpha}/\rho_\alpha W &\equiv S'_{\alpha\alpha} \\ &= -\mathfrak{C}_2\Lambda_\rho(1 - e^{-0.628\Lambda_\rho^{1/2}}) + 0.5e^{-23.75/\Lambda_\rho} ,\end{aligned} \tag{36}$$

$$\begin{aligned}S_{\alpha\alpha\alpha}/\rho_\alpha W^2 &\equiv S'_{\alpha\alpha\alpha} \\ &= -\mathfrak{C}_3\Lambda_\rho(-S'_{\alpha\alpha}/\mathfrak{C}_2\Lambda_\rho)(2.600 + 0.063\ln\Lambda_\rho) ,\end{aligned} \tag{37}$$

where

$$W = Z^2\rho_\alpha/(\rho_e + Z^2\rho_\alpha) ,$$

$$\mathfrak{C}_n = \frac{1}{4n}\frac{(2n-5)(2n-7)\cdots 1}{(2n-4)(2n-6)\cdots 2} , \tag{38}$$

and the ion subscript has been dropped from $\Lambda_{\rho,\alpha\alpha}$. Equations (36) and (37) are accurate to better than 3% for $\Lambda_\rho > 0.5$. By studying the high-density limit of S_4 it appears that a reasonable approximation to the higher S_n is

$$\frac{S_n}{\rho_\alpha W^{n-1}} \equiv S'_n = -\mathfrak{C}_n\Lambda_\rho\left(\frac{-S'_{n-1}}{\mathfrak{C}_{n-1}\Lambda_\rho}\right)^f , \tag{39}$$

where

$$f = (2.600 + 0.063\ln\Lambda_\rho)^{1/(n-2)^{11/12}} . \tag{40}$$

Table I shows a comparison of S_{OCP} obtained from a fit to Monte Carlo data[14] and the result of summing the S_n with $W = 1$ according to Eqs. (36)–(39). Values for both Λ_ρ, the weak-coupling plasma parameter, and $\Gamma = \beta Z^2 e^2/a = (\Lambda_\rho^2/3)^{1/3}$, the strong-coupling parameter are given. The agreement is quite good for small Γ and is within a few percent for higher Γ. The accuracy of the fit given by Eqs. (36)–(39) does not depend on W so that S_{LT} should also be accurate for $W < 1$. It can be shown, using the results of Sec. II F, that degeneracy modifications substantially reduce the electron contributions to W and Λ_ρ when $\theta_e \geq 1$. In partially ionized plasmas more than one type of heavy ion is generally present and an averaging of the S_n for each type of ion is necessary.

Within the framework of the conditions stated above, all terms for $n = 3$ that involve one or more electrons should be small. A method to study the size of these terms when $\Lambda_{\rho,e\alpha}$ and/or

TABLE I. Comparison of the approximate Abe S function with Monte Carlo results.

Λ_ρ	Γ	$-S/\rho$ Abe	$-S/\rho$ Monte Carlo
1	0.693	0.268	0.265
2	1.101	0.493	0.496
3	1.442	0.694	0.704
5	2.027	1.055	1.080
10	3.218	1.877	1.900
20	5.109	3.351	3.287
50	9.410	6.761	6.631
100	14.938	11.136	11.107
500	43.679	35.074	35.381

$\chi_{e\alpha}/\lambda_d$ are large is to use effective potentials, similar to those used in Ref. 10, to solve the hypernetted chain integral equation. The closely related problem for charged hard spheres has recently been studied.[15]

2. *The grand canonical partition function*

The grand canonical partition function is more intricate than the canonical partition function. It was shown in Appendix A of Ref. 7 that the grand canonical partition function and the canonical partition function give different results in regions of mechanical instability. Since the one-component plasma (OCP) is mechanically unstable for $\Gamma > 3.09$, use of $S_{\rm OCP}$ in Eq. (14) will not give the correct $(P_{\rm OCP} - P_0)/\rho kT$. In fact, since negative pressures cannot occur in the grand ensemble, the maximum possible value of $|(P_{\rm OCP} - P_0)/\rho kT|$ obtainable from a one-component nonideal correction is $|-1|$, which is much smaller than the actual $|(P_{\rm OCP} - P_0)/\rho kT|$ for $\Gamma \gg 1$. This dilemma is resolved by keeping the electrons coupled to the ions as the two-component system is mechanically stable to considerably higher densities than the OCP, i.e., substitution of $S(z_e, z_\alpha)$ in Eq. (14) makes it possible to study the grand canonical partition function for high-Z strongly coupled plasmas.

It was described above how the cluster expansion for a reacting gas can be renormalized in terms of an augmented set of activity variables. The resulting cluster expansion has additional terms that were not present in the fundamental particle expansion. These terms are a consequence of the fact that due to the diagrammatic reorganization the Planck-Larkin part of the bound-state partition function is screened. When $Z > 1$ and $\Lambda_{e\alpha} < 1$ the deepest bound states are not much affected by the many-body screening. We note that the sum of the last terms in each curly bracket of Eq. (66) of Ref. 8 is $-U\partial z_{e\alpha}(U)/\partial U$, where $U = z_e + Z^2 z_\alpha$. The sum of the similar terms coming from the fourth cluster coefficients [see Eqs. (75)–(77) of Ref. 8] is $(U^2/2)\partial^2 z_{e\alpha}(U)/\partial U^2$. Collecting all these types of terms together it is found that the activity for one-electron composites is no longer screened, i.e.,

$$z_{e\alpha}(0) = z_{e\alpha}(U) - U\frac{\partial z_e(U)}{\partial U} + \frac{U^2}{2}\frac{\partial^2 z_{e\alpha}(U)}{\partial U^2} - \cdots , \tag{41}$$

and $U = 0$ corresponds to $\lambda_D = \infty$. Equation (27) now reduces to the isolated ion Planck-Larkin form. Continuing this procedure throughout the entire cluster expansion gives an expression in which composites are formally included exactly as fundamental particles. When $\Lambda_{e\alpha} > 1$ the low-lying energy levels become strongly perturbed and an expansion in terms of screened activities becomes essential. However, this also means that high-order $C_{\underline{n}}$ must be calculated for electron-ion interactions. Integral equation methods may be useful in this case.

By reversing each of the steps that lead from Eq. (2) to Eq. (41) of Ref. 8 it is found that, when unscreened activities are used, the S expansion for composite particles also has the same form as for fundamental particles, except the resulting pressure expression is

$$\frac{P}{kT} = \sum_i z_i + S + \sum_i \sum_{m_i=2}^{\infty} \frac{z_i}{m_i!}\left(\frac{\partial}{\partial z_i} z_i\right)^{m_i-2}\left(\frac{\partial S}{\partial z_i}\right)^{m_i} + \tfrac{1}{2}\sum_i \sum_{j\neq i} z_i z_j \left[\psi_{ij} + \frac{1}{2!}\frac{\partial}{\partial z_i}\left(z_i \frac{\partial S}{\partial z_i}\psi_{ij}\right) + \frac{1}{2!}\frac{\partial}{\partial z_j}\left(z_j \frac{\partial S}{\partial z_j}\psi_{ij}\right)\right], \tag{42}$$

where i and j now range over the set $\{z_e, z_\alpha, z_{e\alpha}, z_{ee\alpha}, \ldots\}$, and

$$\psi_{ij} = \left(\frac{\partial S}{\partial z_i}\right)\left(\frac{\partial S}{\partial z_j}\right)\left(\frac{\partial^2 S}{\partial z_i \partial z_j}\right).$$

The terms in Eq. (42) involving ψ_{ij} have not been completely worked out. The $S_{\underline{n}}$'s for terms involving both electrons and ions include only the effective free state parts of the trace, e.g., Eq. (22). Equation (42) is useful for studying the problem of interest.

Consider again the completely ionized plasma with the conditions (29) and (30). Equations (3) and (8) show that the activity is related to ρ and S according to

$$z_i = \rho_i e^{-\partial S/\partial \rho_i}. \tag{43}$$

Substitution of Eqs. (11) and (12) into Eq. (43) shows that $z_e < \rho_e$ and $z_\alpha \ll \rho_\alpha$. As a result, for strong ion coupling, the largest contribution at each m in Eq. (42) comes from the term $z_i(\partial S/\partial z_i)^m/m!$ and has the sum

$$\mathcal{P}_3 = \sum_i z_i\left(e^{\partial S/\partial z_i} - 1 - \frac{\partial S}{\partial z_i}\right), \tag{44}$$

where the subscript of $\mathcal{P}_{r+1}$ indicates that each term involves S at least r times, so that $\mathcal{P}_1 = \sum z_i$ and $\mathcal{P}_2 = S$. The most important terms for $r = 3$ involve factors of the type $(\partial^2 S/\partial z_i^2)(\partial S/\partial z_i)^{m-1}$ and have the sum

$$\mathcal{P}_4 = \frac{1}{2!}\sum_{ij} z_i z_j \frac{\partial^2 S}{\partial z_i \partial z_j}\omega_i \omega_j, \tag{45}$$

where $\omega_\nu = e^{\partial S/\partial z_\nu} - 1$. The $r = 4$ terms have the sum

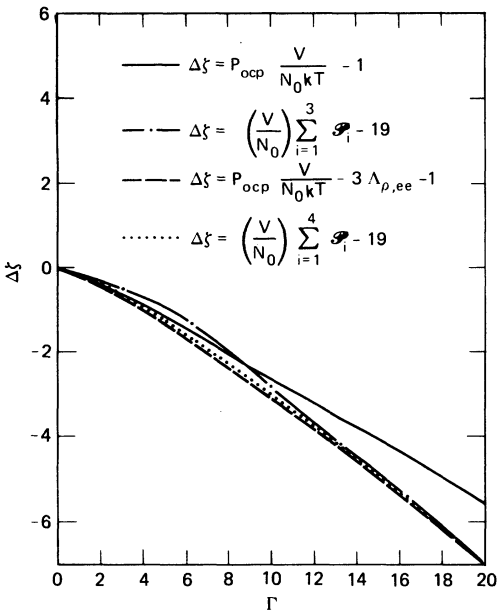

FIG. 1. Nonideal compressibility factor versus Γ for a simplified model of completely ionized Ar. The solid line gives computer simulation results (Ref. 16) for the nonideal compressibility factor of the one-component-plasma (OCP). The dashed line is a similar model, except the electrons are assumed to be distributed according to the Debye-Hückel theory. The dot-dashed line gives the nonideal compressibility factor for the three-term, strongly coupled ion, activity expression, and the dotted line shows results for the four-term activity expression.

$$\mathcal{P}_5 = \frac{1}{3!}\sum_{ijk} z_i z_j z_k \frac{\partial}{\partial z_i}\left(\frac{\partial^2 S}{\partial z_j\,\partial z_k}\,\omega_i\omega_j\omega_k\right). \quad (46)$$

Higher-order terms appear to follow a similar pattern.

An idealized completely ionized Ar plasma is used to study the convergence of the activity expansion in terms of the $\mathcal{P}_{r+1}$. For the sake of simplicity it is imagined that the electron-electron and electron-ion distributions are given by the Debye-Hückel theory but that the ion-ion distribution can be highly correlated. The important contributions due to strong electron-ion attraction are, thus, not considered in this simple model. The reason for choosing this model is that when the conditions (29) and (30) are satisfied, the equation of state is accurately known as a function of ρ and T and can be used to test the convergence of the activity expansion.

Figure 1 compares $\Delta\zeta \equiv (P - P_0)V/N_0kT$ vs $\Gamma = Z^2e^2/akT$, obtained by truncating the activity expansion at $\mathcal{P}_3$ and $\mathcal{P}_4$, respectively, with canonical partition function results. The pressure for the latter is given by $P = P_{OCP} - \rho_e\Lambda_{\rho,ee}/6$, where P_{OCP} was obtained from the Monte Carlo simulations of Hansen[16] and the last term is the electron Debye-Hückel correction. There is a small electron screening correction to P_{OCP} that has not been included. For $kT = Z^2$ Ry, for example, these results should be accurate up to about $\Gamma = 4.8$ ($\Lambda_{\rho,\alpha\alpha} = 18$), since for larger values of Γ the electron-ion plasma parameter ≥ 1. In addition, θ_e and $\gamma_{e\alpha}$ are also approaching unity. As a result the electron corrections are overestimated by this model for large Γ. Large values of Γ are plotted in Fig. 1 to demonstrate that the two-component activity expansion converges properly for $\Gamma > 3.09$. The S function that is used in the activity expression is given by Eq. (34) with density replaced by activity and using the approximate Abe functions given by Eqs. (36)–(39). Electron screening is included in these terms. Figure 1 shows that the activity series truncated after the $\mathcal{P}_3$ term lies close to the density expansion for large Γ but the difference between the two calculations is somewhat greater at intermediate values of Γ. Truncating the activity series after the $\mathcal{P}_4$ term considerably improves the agreement at intermediate values of Γ. Perfect agreement is not expected due to the approximation used to obtain the S_n and the neglect of electron screening in P_{OCP}.

F. Quantum statistical corrections to the activity expansion

The theory discussed so far has assumed Boltzmann statistics so that F_0 in Eq. (8) is the free energy of an ideal Boltzmann gas. If degeneracy modifications to F_0 are treated as a nonideal contribution and included in the definition of S, Eq. (14) remains valid. In addition to the ideal gas modifications there are also degeneracy and exchange modifications to S itself. The free energy is now given by

$$(F - F_0)/VkT = -S_f, \quad (47)$$

where

$$S_f = \Delta F_0/VkT + S + \Delta S, \quad (48)$$

$$\frac{\Delta F_0}{VkT} = \rho_e[\beta\mu_e - \mathfrak{F}_{3/2}(\beta\mu_e)/y] + \rho_\alpha(\beta\mu_\alpha - 1) - \frac{F_0}{VkT}, \quad (49)$$

$\mathfrak{F}_n$ is a Fermi function, $y = \mathfrak{F}_{1/2}(\beta\mu_e) = \lambda_e^3\rho_e/(2s+1)$, μ_e and μ_α are the chemical potentials for the noninteracting system, and ΔS is the quantum statistical correction to the S function.

In the ring approximation it has been shown that[17]

$$S_R + \Delta S = 1/12\pi\lambda_D^3, \quad \lambda_D = \{4\pi\beta e^2[I_{-1/2}(\beta\mu_e) + Z^2\rho_\alpha]\}^{1/2}, \quad (50)$$

where

$$I_{-1/2}(\beta\mu_e) \equiv (2s+1)\mathfrak{F}_{-1/2}(\beta\mu_e)/\lambda_e^3.$$

Using the relations[18]

$$e^{\beta\mu_e} = y\left[1 + \frac{1}{2^{3/2}}\, y + \left(\frac{1}{4} - \frac{1}{3^{3/2}}\right)y^2 + \cdots\right] \tag{51}$$

and

$$\mathfrak{F}_\nu(\beta\mu) = \sum_{r=1}^{\infty} (-1)^{r+1} e^{r\beta\mu} r^{-(\nu+1)}, \tag{52}$$

it is easy to show that the leading degeneracy corrections to F_0 and S are

$$\frac{\Delta F_0}{VkT} = -\frac{1}{2^{5/2}}\left(\frac{\lambda_e^3}{(2s+1)}\right)z_e^2 + \left(\frac{1}{3^{5/2}} - \frac{1}{2^4}\right)\left(\frac{\lambda_e^3}{2s+1}\right)^2 z_e^3 + \cdots, \tag{53}$$

$$\Delta S = -\frac{1}{2^{3/2}}\left(\frac{\lambda_e^3}{2s+1}\right)\left(\frac{\partial S_R}{\partial z_e}\right)z_e^2 + \cdots. \tag{54}$$

Densities have been replaced by activities in Eqs. (53) and (54) since it is $S(z_e, z_\alpha)$ that appears in Eq. (14). In addition to the degeneracy corrections there are also exchange corrections. Two-electron exchange corrections to S_{ee} can be calculated from the phase shifts of the Debye potential.[7,19]

The analysis leading to Eq. (14) of Ref. 8 could be repeated using S_f, the quantum statistical form of S just described. Alternatively, the method of Cooper and DeWitt[17] can be used to modify specific diagrammatic sums in the grand canonical partition function that lead to individual terms in Eq. (19). The rule is that for each particle in a diagram a statistical factor $\mathfrak{F}_m = I^{(\beta\mu)}_{-m+3/2}$ is introduced, where m is the number of interaction lines that link the particle. Since two interaction lines link each particle in a ring diagram, it follows immediately that $S_R(z_e + Z^2 z_\alpha) \to S_R(I_{-1/2}(\beta\mu_e) + Z^2 z_\alpha)$. Similarly all particles in the chains that replace the Coulomb potential with the screened Coulomb potential are linked by two interaction lines so that $\lambda_D(z_e + Z^2 z_\alpha)$ is replaced everywhere by $\lambda_D(I_{-1/2}(\beta\mu_e) + Z^2 z_\alpha)$.

Consider next the "two-beaded-string-diagrams" that lead to the third term in Eq. (19). The one-component set of these diagrams in which particles are sequentially added to the right bead is shown in Fig. 2. According to the Cooper-DeWitt rule,[17] a factor $I_{-1/2}$ is introduced for every particle except the one that connects the beads for which a factor $I_{-5/2}$ is introduced. Summation of the diagrams shown in Fig. 2 gives

FIG. 2. Set of reducible classical diagrams that contribute terms of order z^2 to the activity expansion.

$$g_1 = \tfrac{1}{2}\beta_1^R I_{-1/2} I_{-5/2} \sum_{j=2}^{\infty} (I_{-1/2})^{j-1} \beta_{j-1}^R = \tfrac{1}{2}\beta_1^R I_{-1/2} I_{-5/2} \frac{\partial S_R(I_{-1/2})}{\partial I_{-1/2}}, \tag{55}$$

where β_j^R is the ring approximation to an irreducible cluster integral. By putting two, three, etc. particles in the left bead and repeating the process, it is established that

$$g = \tfrac{1}{2} I_{-5/2}\left(\frac{\partial S_R(I_{-1/2})}{\partial I_{-1/2}}\right)^2. \tag{56}$$

Consider next the fourth term in Eq. (19). There are two basic types of diagrams that contribute to this term, "the three-beaded-string diagrams," and the "three-leaf-clover diagrams." In the classical Boltzmann limit the lowest order of these diagrams all contribute a factor β_1^3. This is not the case, however, for Fermi statistics. Figure 3 shows a few of these diagrams. We first sum the rightmost bead and leaf. The cloverleaf diagrams have one particle that is linked by six interactions while the three-beaded-string diagram has one particle in the right bead that is lined by four lines so that the sum becomes

$$h_1 = \tfrac{2}{3}\beta_1^2 I_{-1/2}^2 (\tfrac{3}{4} I_{-5/2} + \tfrac{1}{4} I_{-9/2}) \frac{\partial S_R(I_{-1/2})}{\partial I_{-1/2}}. \tag{57}$$

Summation over the remaining diagrams gives

$$h = \frac{1}{3!}(\tfrac{3}{4} I_{-5/2}^2 / I_{-1/2} + \tfrac{1}{4} I_{-9/2}) \frac{\partial}{\partial I_{-1/2}}\left[I_{-1/2}\left(\frac{\partial S_R}{\partial I_{-1/2}}\right)^3\right]. \tag{58}$$

Generalization to two components is straightforward, e.g., the two-component two-beaded-string diagrams give

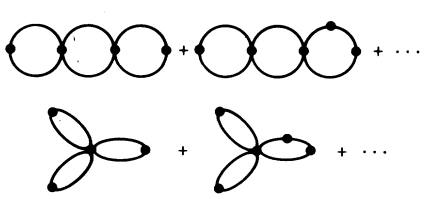

FIG. 3. Two types of reducible classical diagrams that contribute terms of order $z^{5/2}$ to the activity expansion.

$$g=\frac{1}{2!}I_{-5/2}\left(\frac{\partial S_R(I_{-1/2}+Z^2z_\alpha)}{\partial I_{-1/2}}\right)^2 + \frac{1}{2!}z_\alpha\left(\frac{\partial S_R(I_{-1/2}+Z^2z_\alpha)}{\partial z_\alpha}\right)^2 . \quad (59)$$

When $\theta_e \to 0$, $I_{-m/2} \to z_e$, and Eq. (59) reduces to a form obtained in Ref. 7.

Cooper and DeWitt[17] have given degeneracy corrections to the three-rung-ladder diagram, which yield the leading high-temperature correction to C_2. Consider finally terms like $z_e(\partial S_R/\partial z_e)(\partial C_2/\partial z_e)$. The factor $\partial S_R/\partial z_e$ results from a many-body sum over ring type diagrams while $\partial C_2/\partial z_e$ is a screened two-body diagram. Figure 4 shows the classical form of these diagrams where the triple lines represent the sum $\sum_{m=3}^{\infty}(-\beta V)^m/m!$ In the final result the sum over the classical ladder diagrams will be replaced by a Slater sum. These diagrams introduce coupling between the plasma and composite particles. Putting degeneracy corrections in for all the particles except the two connected by triple lines, i.e., ladder diagrams having $m>2$, gives for two components

$$u=z_e\left(\frac{S_R(I_{-1/2}+Z^2z_\alpha)}{\partial I_{-1/2}}\right)\frac{\partial C_2}{\partial z_e} + z_\alpha\left(\frac{\partial S_R(I_{-1/2}+Z^2z_\alpha)}{\partial z_\alpha}\right)\frac{\partial C_2}{\partial z_\alpha} . \quad (60)$$

Degeneracy can be put in still more complicated types of diagrams. The final result of this is that the rearrangement of the C expansion done in Ref. 8 to incorporate composite particles carries through without change so that Eq. (41) of that paper becomes

$$\frac{P}{kT}=I_{3/2}+z_\alpha+z_{e\alpha}\cdots + S_R(I_{-1/2}+Z^2z_\alpha+(Z-1)^2z_{e\alpha}\cdots) + g^*+h^*+C_2^*+u^*, \quad (61)$$

where g^*, h^*, and u^* are multicomponent (including composite particles) generalizations of Eqs. (56), (58), and (60), respectively. C_2^* involves both fundamental and composite particles with only effective scattering-state parts of electron-ion components included. The composite particle activities in Eq. (61), as described above, are not screened. It is noted that Eq. (61) shows that e-e and e-i terms are strongly suppressed by electron degeneracy, which tends to keep the electrons from becoming strongly coupled as the density is increased. The S expansion that was used in Sec. II E for strong ion coupling is somewhat complicated by degeneracy. The Φ_3 term, for example, is no longer given by Eq. (44). The electron component of Φ_3 is given approximately by

$$I_{-5/2}\left(e^{\partial S/\partial I_{-1/2}}-1-\frac{\partial S}{\partial I_{-1/2}}\right). \quad (62)$$

The cloverleaf and ladder-type diagrams, however, introduce factors other than $I_{-5/2}$ so that the correct function is more complicated than Eq. (62). For applications involving strong ion coupling to be discussed in the next section the electrons will be only slightly degenerate, so that the approximation of Eq. (62) is adequate.

FIG. 4. Set of classical diagram that contributes terms of order $z^{5/2}$ for point charges. The quantum-mechanical version of this diagram contributes terms of order $z^{3/2}$ for composite particles.

III. CALCULATION OF THE EQUATION OF STATE OF ARGON

A. Energy levels and phase shifts

To evaluate thermodynamic properties of strongly coupled reacting plasmas using the results of Sec. II requires a large computer code which is referred to as ACTEX. In order to calculate composite particle activities it is necessary to obtain multielectron energy levels. Calculation of multiparticle scattering-state phase shifts is also required.[19] This is accomplished through the introduction of effective two-particle potentials composed of a pseudo-Debye screened long-range part (with λ_D^* defined in terms of activities) and exponential screened Coulomb terms for each shell of core electrons[20] according to

$$V(Z,r,\lambda_D^*)=-2\left((Z-\nu)e^{-r/\lambda_D^*}+\sum_{n=1}^{n^*}N_ne^{-\alpha_nr}\right)\Big/r, \quad (63)$$

where ν is the number of electrons for the parent ion, N_n is the number of electrons in the shell having principle quantum number n, and α_n is the corresponding screening parameter. The potential $V(Z,r,\lambda_D^*)$ is valid when $\tau<1$ and $\gamma_{e\alpha}<1$. To first approximation the electron-ion potentials yield via electrostatics the ion-ion potentials.[8] The core part of the ion-ion potentials are most important for low degrees of ionization since otherwise the strong repulsion coupled with reduced ion size keeps the cores from overlapping. As a result more accurate

potentials are used for neutral-neutral and ion-neutral interactions. For Ar-Ar interactions the potential given by Ross *et al.*[21] is used and for Ar^+-Ar interactions the potential given by DeVoto[22] is used. For e-Ar interactions a potential of the form (63) with a polarization correction of the form $\alpha/(C+r^4)$ was adjusted to fit experimental momentum-transport cross-section data.[23]

B. Numerical results

For multicomponent plasmas it is useful to define an average density-dependent plasma parameter

$$\bar{\Lambda}_\rho = \langle \xi^2 \rangle e^2/kT\lambda_d^* , \tag{64}$$

where

$$\langle \xi^2 \rangle = \sum_i \xi_i^2 \rho_i \Big/ \sum_i \rho_i ,$$

is the average of ξ^2 for all species. For large ξ, $\bar{\Lambda}_\rho \ll \Lambda_{\rho,\text{ions}}$, but it is a more appropriate measure of the importance of plasma interactions on the equation of state. Neutrals have been included in $\bar{\Lambda}_\rho$ to more accurately reflect the importance of nonideality in the equation of state, i.e., errors resulting from use of a low-order theory to treat slightly ionized, but very nonideal plasmas, do not substantially effect the total pressures and energies. Figure 5 shows constant $\bar{\Lambda}_\rho$ contours in density-temperature space. The area to the left of the $\bar{\Lambda}_\rho = 0.2$ contour is a region of slight nonideality which can be treated by a Saha-Debye-Hückel approach. The temperature-density space for which $0.2 \leq \bar{\Lambda} \leq 3.5$ is a region of moderate nonideality. The $\bar{\Lambda}_\rho = 3.5$ contour is near the limit of validity of the present theory since, in the activity expansion, $\Lambda_{e\alpha}$ for the dominant species is approximately equal to 1. In the rightmost area even the electrons are becoming strongly coupled in the slightly degenerate high-temperature region. For densities in the vicinity of 1 g/cm^3 and kT less than 5-eV argon is a strongly repulsive fluid and the plasma parameter is not the primary measure of nonideality. The approximate region where third virial core interactions become important is indicated by the dashed line. A fluid perturbation-theory approach can be used in the high-density low-temperature region.[21]

Figure 6 is a three-dimensional plot of PV/N_0kT versus temperature and density. Results from the fluid perturbation-theory method[21] have also been included. The two data sets were matched up by a cubic spline interpolation across a gap $\Delta\rho/\rho \approx 0.5$ centered on the dashed line indicated in the figure. The lines are selected isochores and isotherms from the final database. The relative smoothness of the isochores indicates that the two sets of data are compatible. The density dependence of the plateaus separating the L and M shells and the K and L shells is evident along the 28- and 255-eV isotherms, respectively. The increase in PV/N_0kT as kT is lowered at high density is due to the repulsive interactions between Ar-Ar, Ar^+-Ar, and Ar^+-Ar^+. Pressure ionization and electron degeneracy will both enhance this characteristic at densities higher than those considered here.

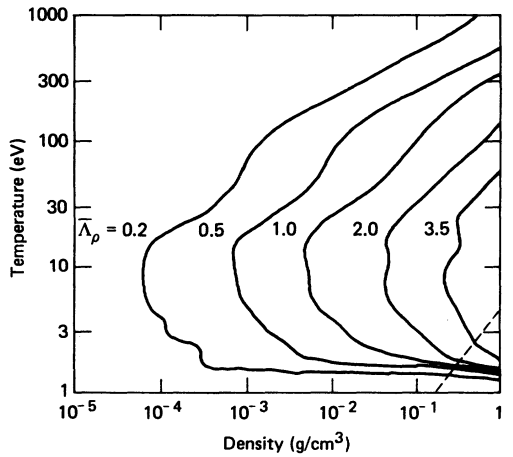

FIG. 5. Contours of constant lambda in (T, ρ) space. The region to the right of the dashed line requires at least third virial type corrections for core-core interactions.

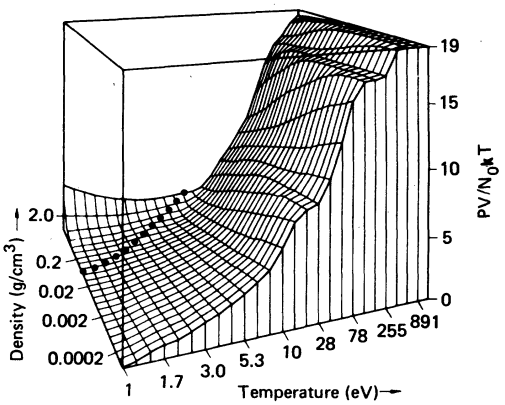

FIG. 6. Three-dimensional plot of PV/N_0kT for Ar as a function of T and ρ. The dotted line indicates approximately where core repulsion becomes important.

Figure 7 displays PV/N_0kT vs T for Ar at a density of 0.1 g/cm^3. Results for the ideal gas, $PV/N_0kT = \Phi_1$, and $PV/N_0kT = (V/N_0)(\Phi_1 + \Phi_2 + \Phi_3)$ approximations to the pressure are shown. The calculation is valid along most of the isochore, except $\Lambda_{e\alpha}$ is somewhat larger than unity for temperatures between 1.5 and 3.5 eV ($\Lambda_{e\alpha}$ has a maximum value of 1.42 at a temperature of 2.18 eV). The difference between the ideal gas and the three-term pressure approximations is typically 10%, which is much smaller than predicted by the Debye-Hückel theory, e.g., in the Debye-Hückel theory $PV/N_0kT = (N/N_0)(1 - \bar{\Lambda}_\rho/6)$ and $\bar{\Lambda}_\rho \approx 2.8$ in the 5–10-eV temperature range. Inclusion of the Φ_4 term has a relatively small effect on the pressure and the four-term pressure equation is, therefore, not included in the comparison. The total moles of particles, N/N_0, predicted by the three-term pressure equation is also plotted in Fig. 7. Since it lies above the ideal gas curve the effect of interactions is actually somewhat greater than indicated by the small difference between the two approximations to the pressure. At low T the core repulsions become more important than Coulomb attractions

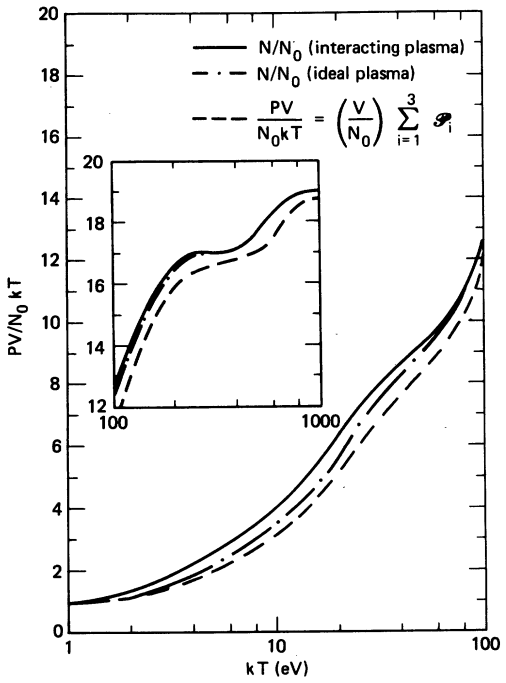

FIG. 7. PV/N_0kT vs kT for Ar having $\rho = 0.1$ g/cm^3. The solid line gives N/N_0 for the interacting system. The dot-dashed line gives N/N_0 for the noninteracting system, i.e., the Saha equation. The dashed line gives the compressibility factor for the three-term activity series.

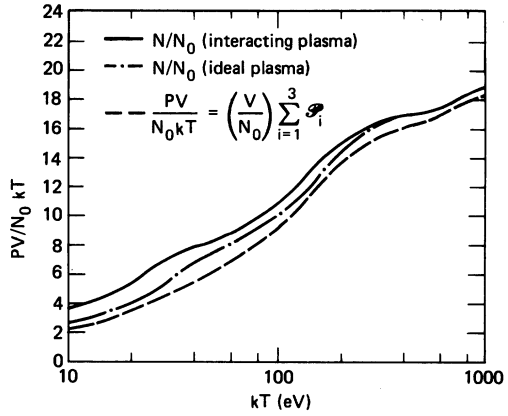

FIG. 8. Same as Fig. 7 except $\rho = 1.0$ g/cm^3.

so that N/N_0 is slightly smaller than PV/N_0kT. Core repulsion partially offsets Coulomb attraction at intermediate values of the temperature.

Figure 8 is similar to Fig. 7 except that the density has been increased to 1 g/cm^3. The differences between the ideal gas and three-term pressure equation compressibility factors are typically 20%, while N/N_0 in the presence of the corresponding interactions is as much as 30% greater than it is in the ideal limit. $\Lambda_{e\alpha}$ is ≥ 1 for $kT < 40$ eV and increases slowly to 1.58 at $kT = 15$ eV, i.e., the lowest-lying energy levels are becoming strongly perturbed so that an expansion in terms of isolated ion energy levels is not appropriate. The packing fraction is also increasing rapidly for $kT < 40$ eV as substantial numbers of electrons are becoming bound in the M shell. Both of these effects will increase the pressure so that the error introduced by neglecting high-order terms may be large. The Debye length (in terms of activity) at $kT = 40$ eV is $3.29a_0$, which is somewhat greater than the mean core radius ($1.2a_0$) for Ar^{5+}, the dominant ionic species. It is noted that the effective potential that enters the density expansion is of somewhat shorter range since the Debye length in terms of densities is $1.00a_0$ at $kT = 40$ eV. This is due to the fact that the activity expansion gives screening for interacting particles while the density expansion gives screening for randomly distributed particles. As expected, Coulomb coupling decreases the screening.

Figure 9 shows $C_V/19k$ vs kT. For $kT > 1500$ eV Ar is completely ionized and weakly coupled, so that $C_V/19k \rightarrow \frac{3}{2}$, the ideal gas result. However, there are pronounced peaks in $C_V/19k$ for $kT < 1000$ eV. The peaks in the 600–900-eV range are associated with the filling of the K

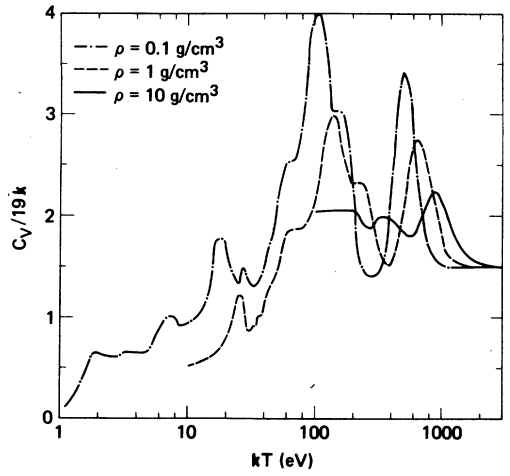

FIG. 9. $C_V/19k$ vs kT for Ar at several densities.

shell. Peaks in $C_V/19k$ in the 100–300-eV range are associated with the filling of the L shell. Owing to the wider spread in energy levels for nearly neutral ions the M-shell filling does not show pronounced peaks. The small peaks in the 7–30-eV range are apparently associated with small energy gaps between subshells. At low density the specific heats in the reaction zones are much higher than the corresponding values for an ideal gas.

C. Comparison with experiment

Shock wave experiments on gaseous Ar which achieve final states in the plasma regime have been reported by Christian and Yarger[24] and by Gryaznov *et al.*[25] and references therein. Table II gives a comparison of the present work with the Christian-Yarger and the Gryaznov *et al.* experiments. Choosing H and V as the independent variables, the dependent variable is the pressure. N_e/N_0 is the fractional ionization of the $3p^6$ state. Differences between PV/N_0kT-1 and N_e/N_0 are due to interaction corrections, which even at this low density are somewhat smaller than predicted by the Debye-Hückel theory. The largest experimental uncertainty is in the volume which is estimated at 5% by Christian and Yarger and 7–19% by Gryaznov *et al.* Additional uncertainties of a few percent also exist in the measured value of H. Accepting the measured values of V and H and attributing all the error to the pressure (solely for the purposes of this comparison) gives an uncertainty of 6–7% for the Christian and Yarger experiments and 10–22% for the Gryaznov *et al.* experiments. The calculated and measured pressure agree within the estimated experimental uncertainty except for one data point. Gryaznov *et al.* give data for which $\Lambda_{e\alpha}>1$ that has not been included in Table II. Shock experiments on liquid Ar which achieve final states in the partially ionized dense fluid regime have also recently been reported.[21] The fluid perturbation theory is in very good agreement with these experiments.

IV. CONCLUDING REMARKS

This paper has given a theoretical basis for going beyond intuitive model approaches for obtaining the equation of state of partially de-

TABLE II. Comparison of theory and experiment for Ar.

Experiment			Theory (Constant H,V)				
V (cm^3/g)	P (10^2 MPa)	H (MJ/kg)	P (10^2 MPa)	T (10^3 K)	N_e/N_0	$\bar{\Lambda}_\rho$	P_{theory}/P_{expt}
			Christian and Yarger (Ref. 24)				
166.8	0.154	0.0725	0.158	12.4	0.017	0.01	1.03
153.7	0.168	0.0808	0.185	13.1	0.027	0.02	1.10
134.6	0.300	0.1407	0.283	17.1	0.156	0.16	0.94
118.2	0.314	0.1374	0.320	17.1	0.149	0.18	1.02
101.8	0.441	0.1915	0.444	18.5	0.215	0.31	1.01
91.7	0.492	0.2127	0.523	19.2	0.258	0.34	1.06
80.3	0.813	0.3383	0.793	22.6	0.472	0.58	0.98
81.8	0.848	0.375	0.843	23.7	0.490	0.67	0.99
			Gryaznov *et al.* (Ref. 25)				
86.0	0.692	30.1	0.692	21.8	0.445	0.56	1.00
87.0	0.597	20.9	0.551	19.1	0.24	0.33	0.92
25.0	2.73	31.1	2.59	24.1	0.477	0.99	0.95
18.8	2.96	20.9	2.68	20.6	0.238	0.58	0.91

generate, strongly coupled, reacting plasmas. By concentrating on the underlying analytic structure rather than a diagrammatic study of various orders of approximation, it has been possible to derive an activity expression which simultaneously treats ionization equilibrium and strong heavy-ion coupling. This work has many applications in applied problems of current interest. The results presented here are representative of the type of data that can be generated. It is anticipated that in the future this work will be extended so that the restrictions outlined in Sec. I can be relaxed and that the general approach will be extended to include nonequilibrium properties.

ACKNOWLEDGMENT

The author wishes to thank E. T. Florance for helpful discussions and encouragement of this work. Useful discussions with H. E. DeWitt and D. Mukherjee are also gratefully acknowledged. I am indebted to M. Ross for providing his fluid perturbation-theory calculations for Ar. G. L. Haggin provided considerable assistance with the computer codes. This work was performed under the auspices of the U. S. Department of Energy by Lawrence Livermore National Laboratory under Contract No. 7405-Eng-48, and supported in part by the Office of Naval Research.

[1]Stephen G. Brush, *Progress in High Temperature Physics and Chemistry*, edited by C. A. Rouse (Pergamon, Oxford, 1967), Vol. 1, p. 1.
[2]W. Ebeling, W. D. Kraeft, and D. Kremp, *Theory of Bound States and Ionization Equilibrium in Plasmas and Solids* (Akademie-Verlag, Berlin, 1977).
[3]W. Ebeling, Physica 73, 573 (1974).
[4]Yu. G. Krasnikov and V. I. Kucherenko, Teplofiz, Vys. Temp. 16, 43 (1978).
[5]Yu. G. Karsnikov, Zh. Eksp. Teor. Fiz. 73, 516 (1977) [Sov. Phys.—JETP 46, 270 (1977)].
[6]H. E. DeWitt and F. J. Rogers, Phys. Earth Planet. Inter. 6, 51 (1972).
[7]F. J. Rogers and H. E. DeWitt, Phys. Rev. A 8, 1061 (1973).
[8]F. J. Rogers, Phys. Rev. A 10, 2441 (1974).
[9]F. J. Rogers, Phys. Lett. 61A, 358 (1977).
[10]F. J. Rogers, Phys. Rev. A 19, 375 (1979).
[11]R. Abe, Prog. Theor. Phys. (Kyoto) 22, 213 (1960).
[12]H. E. DeWitt, J. Math. Phys. 7, 161 (1966).
[13]S. G. Brush, H. E. DeWitt, and J. G. Trulio, Nucl. Fusion 3, 5 (1963).
[14]Hugh E. DeWitt, in *Strongly Coupled Plasmas*, edited by Gabor Kalman and Paul Carini (Plenum, New York, 1978).
[15]F. J. Rogers, J. Chem. Phys. 73, 6272 (1980).
[16]J. P. Hansen, Phys. Rev. A 8, 3096 (1973).
[17]M. S. Cooper and H. E. DeWitt, Phys. Rev. A 8, 1910 (1973).
[18]Richard Tolman, *The Principles of Statistical Mechanics* (Oxford University Press, London, 1938).
[19]F. J. Rogers, Phys. Rev. A 4, 1145 (1971).
[20]F. J. Rogers, Phys. Rev. A 23, 1008 (1981).
[21]M. Ross, W. Nellis, and A. Mitchell, Chem. Phys. Lett. 68, 532 (1979); M. Ross, J. Chem. Phys. 73, 4445 (1980).
[22]R. S. DeVoto, Phys. Fluids 16, 616 (1972).
[23]H. B. Millary, R. W. Crampton, J. A. Rees, and A. G. Robertson, Aust. J. Phys. 30, 61 (1977).
[24]R. H. Christian and F. L. Yarger, J. Chem. Phys. 23, 2042 (1955).
[25]V. K. Gryaznov, M. V. Zhernokletov, V. N. Zubarev, I. L. Iosilevskii, and E. Tortov, Zh. Eksp. Teor. Fiz. 78, 573 (1980) [Sov. Phys.—JETP 51, 288 (1980)].